SIMPLE MODEL OF LATTICE DYNAMICS FOR MAGNESIUM, COBALT AND YTRIUM

By A. Czachor

Institute for Nuclear Research, Świerk*

And A. Rajca

Institute for Experimental Physics, Warsaw University**

(Received October 3, 1970)

A simple model of lattice dynamics for hexagonal, close-packed structure crystals is proposed. Parameters of the model can be derived from the elastic constants data. The model was successfully tested by evaluating phonon frequencies for magnesium, and comparing them with experimental ones. Using the model, phonon dispersion curves and frequency spectra for magnesium, cobalt and ytrium are calculated.

Introduction

Phonon dispersion curves for hexagonal, close-packed (hcp) structure metals Be, Mg and Zn have been measured at room temperatures some years ago [1–5] and many theoretical treatments of these results, both phenomenological and "from first principles" have been published [6–10]. However, the lattice dynamics of many other hcp metals is still unknown, but only in the acoustic $\vec{q} \to 0$, $\omega \to 0$ limit (the elastic constants). It seems interesting to try obtaining more information about the phonon spectrum for these metals by a proper extrapolation of the acoustic limit information to other $(\vec{q}, \omega)$ regions.

A simple model of the Born–v. Karman type for the lattice dynamics of hexagonal, close-packed structure is presented below. The main advantage of the model is that its parameters can be fixed by using all the elastic constants and the elastic constants only. The model works relatively well for magnesium, and one can expect it to work well also for cobalt and ytrium. The model was partly suggested by the results of Champier and Touissant [11].

* Address: Instytut Badań Jądrowych, Świerk k. Otwocka, Poland.
** Address: Instytut Fizyki Doświadczalnej UW, Warszawa, Hoża 69, Poland.

Description of the model

All five elastic constants of the hcp structure can be in general expressed as non-linear combinations of force constants of the Born–v. Karman theory [12]. There exists also an interrelation between force constants, the so-called Huang condition for the absence of nonisotropic internal stresses. Using these six equations one can determine no more than six force constants. They are just six, if the equations are linear and consistent.

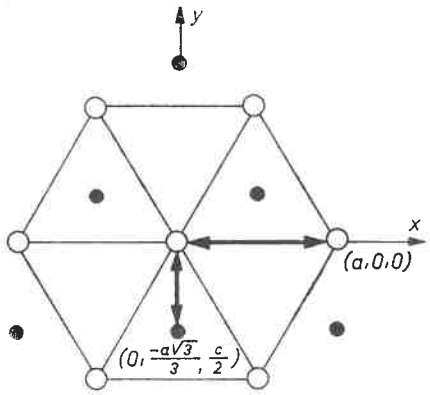

Fig. 1. Projection of the hcp structure on the basal plane and the scheme of interactions for the model discussed

A following model yields a set of equations which underlie these conditions (Fig. 1, Table I):

i. Interactions of a general type with nearest neighbours in the basal plane $z = 0$.

ii. "Quasi-central" force matrix for interactions with nearest neighbours in the adjacent, $z = \pm\frac{c}{2}$ planes. This resembles a central forces matrix because the xx-diagonal force constant is assumed equal to 0, but the remaining force constants B, G, D are symmetry-restricted only.

TABLE I

Position of the representative atom of a coordination sphere	Indices in the scheme of paper [12]	Force matrix in the model presented
$\begin{bmatrix} a \\ 0 \\ 0 \end{bmatrix}$	$k = 0$ $l = 1$ $m = 0$	$-\begin{bmatrix} a & f & 0 \\ -f & b & 0 \\ 0 & 0 & g \end{bmatrix}$
$\begin{bmatrix} 0 \\ \frac{-a\sqrt{3}}{3} \\ \frac{c}{2} \end{bmatrix}$	$K = 0$ $L = 0$ $M = 0$	$-\begin{bmatrix} 0 & 0 & 0 \\ 0 & B & D \\ 0 & D & G \end{bmatrix}$

The antisymmetric force constant f cannot be fixed from the elastic constants alone, for it does not appear in the corresponding equations. We have left it in the formulas for

elements of dynamical matrix, because it represents interesting many-bodyforces (f becomes equal to zero when only two-particle ion-ion interaction potentials occur).

The elastic constants and the Huang condition can be written as follows (see [12])

$$c_{11} = \frac{\sqrt{3}}{2c} \cdot \left(3 \cdot a + b + \frac{2}{3} \cdot B\right)$$

$$c_{33} = \frac{\sqrt{3}c}{a^2} \cdot G$$

$$c_{44} = \frac{2}{\sqrt{3}c} \cdot (3 \cdot g + G)$$

$$c_{66} = \frac{\sqrt{3}}{2c} \cdot (a + 3 \cdot b)$$

$$c_{13} + c_{44} = \frac{2}{a} \cdot D$$

$$\frac{3}{4} \cdot \left(\frac{c}{a}\right)^2 \cdot B = 3 \cdot g + G.$$

As a solution one obtains

$$a = \frac{\sqrt{3}c}{4} \cdot c_{11} - \frac{1}{2\sqrt{3}} \cdot \frac{a^2}{c} \cdot c_{44} - \frac{c}{4\sqrt{3}} \cdot c_{66}$$

$$b = \frac{\sqrt{3}c}{4} \cdot c_{66} + \frac{1}{6\sqrt{3}} \cdot \frac{a^2}{c} \cdot c_{44} - \frac{c}{4\sqrt{3}} \cdot c_{11}$$

$$g = \frac{c}{2\sqrt{3}} \cdot \left(c_{44} - \frac{2}{3} \cdot \left(\frac{a}{c}\right)^2 \cdot c_{33}\right)$$

$$B = \frac{2a^2}{\sqrt{3}c} \cdot c_{44}$$

$$G = \frac{a^2}{\sqrt{3}c} \cdot c_{33}$$

$$D = \frac{a}{2} \cdot (c_{13} + c_{44}).$$

The elements of the dynamical matrix are given in the Appendix and phonon dispersion formulae can be found in [21]. In this simple model the following equation holds (group theory classification of phonon modes is according to Iyengar *et al.* [2] and Pynn and Squires [3]):

$$\frac{\omega(\Gamma_3^+)}{\omega(\Gamma_5^+)} = \sqrt{\frac{c_{33}}{c_{44}}}.$$

If purely central interactions ($g = 0$) and ideal hcp structure $\left(\frac{c}{a} = \sqrt{\frac{8}{3}}\right)$ are assumed, the Huang condition predicts:

$$\frac{c_{33}}{c_{44}} = 4.$$

Phonon dispersion curves

The model was tested by calculating force constants and phonon frequencies for Be, Mg and Zn, and comparing them with experimental data. A satisfactory fit was obtained only for magnesium (Figs 2, 3). Optical frequencies at $\vec{q} = 0$ fit experimental values very well: $\omega(\Gamma_3^+) = 4.59_{10}13$ rad/sec, $\omega(\Gamma_5^+) = 2.37_{10}13$ rad/sec.

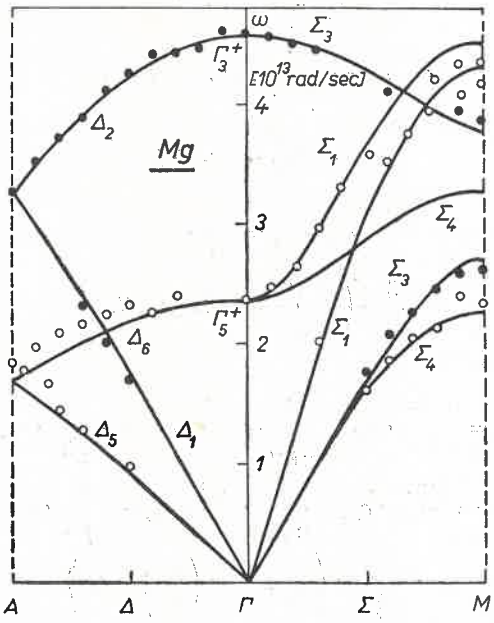

Fig. 2. Phonon dispersion curves in the directions Δ and Σ for Mg. Points — experimental data of Iyengar *et al.* [2]. Lines — model discussed

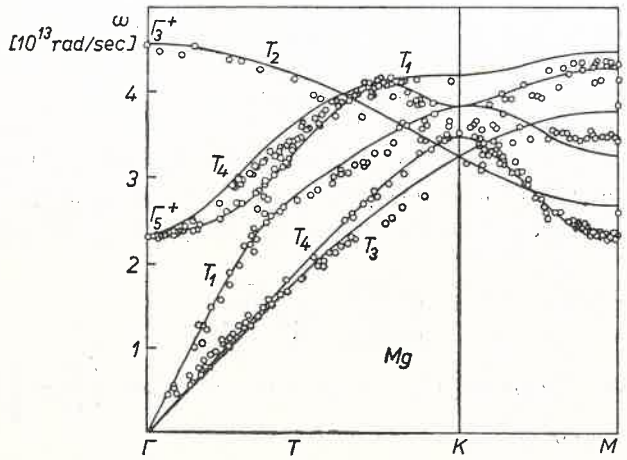

Fig. 3. Phonon dispersion curves in the direction T for Mg. Points — experimental data of Squires and Pynn [3], at Γ and M — data of Iyengar *et al.* [2]. Lines — model discussed

In fact, for Mg the present model fits the experiment nearly as well as the Iyengar's axial symmetry model and the four-nearest-neighbours general force model, where some force constants were found by least-square fitting to experimental phonon frequencies [2], and the three-nearest-neighbours general force model of Squires [3]. For the direction T the agreement of our model with experiment is somewhat worse, although the discrepancies do not exceed ~5%. For branches T_2 and T_4 acoustic the agreement is still good.

There is also another, more sophisticated model of lattice dynamics of Mg, based on the elastic constants only [7]. The interactions with 4 nearest neighbours and the contribution of electronic bulk modulus to lattice dynamics are taken into account. In spite of greater complexity, the agreement of calculated dispersion curves with experiment is not better than in our case and for some phonon frequencies (ex. $\omega(\Gamma_3^+)$— slightly worse.

The ratios of elastic constants, c_{44}/c_{66} and c_{33}/c_{11} for Mg are nearly equal to one, which is characteristic for isotropic media. Also the ratio c/a for magnesium (1.62) is close to the c/a ratio for ideal hcp structure (1.633). As may be seen (Table II), the same is true also

TABLE II

Lattice constants (Å) and elastic constants (10^{11} dyn/cm^2)

	Mg	Co	Y
a	3.2028	2.51	3.65
c	5.196	4.07	5.73
c_{11}	5.964	30.07	7.79
c_{33}	6.164	35.81	7.69
c_{66}	1.702	7.1	2.47
c_{44}	1.642	7.55	2.43
c_{13}	2.104	10.27	5.51

(Elastic constants for Mg and Co from [14], for Y from [15]).

TABLE III

Force constants (dyn/cm) for Mg, Co and Y

a	b	g	B	G	D
Mg $1.12_{10}4$	$-3.31_{10}2$	$1.21_{10}2$	$3.74_{10}3$	$7.03_{10}3$	$6.06_{10}3$
Co $4.55_{10}4$	$-4.03_{10}3$	$-1.80_{10}3$	$1.35_{10}4$	$3.20_{10}4$	$2.24_{10}4$
Y $1.57_{10}4$	$2.30_{10}2$	$5.79_{10}2$	$6.52_{10}3$	$1.03_{10}4$	$8.27_{10}3$

for cobalt and ytrium. Assuming that these macroscopic similarities reflect some analogies in their microscopic interactions, one can expect similarities in other properties too. Based on this assumption, the force constants and phonon dispersion curves for Co and Y were calculated (Table III, Figs 4, 5). The optical frequencies at $\vec{q} = 0$, $\omega(\Gamma_3^+)$, $\omega(\Gamma_5^+)$ are as follows (the unit- rad/sec):

$$\text{Co: } 6.23_{10}13,\ 2.86_{10}13;\ \text{Y: } 2.61_{10}13,\ 1.47_{10}13.$$

At present there are no experimental data to be compared with these values.

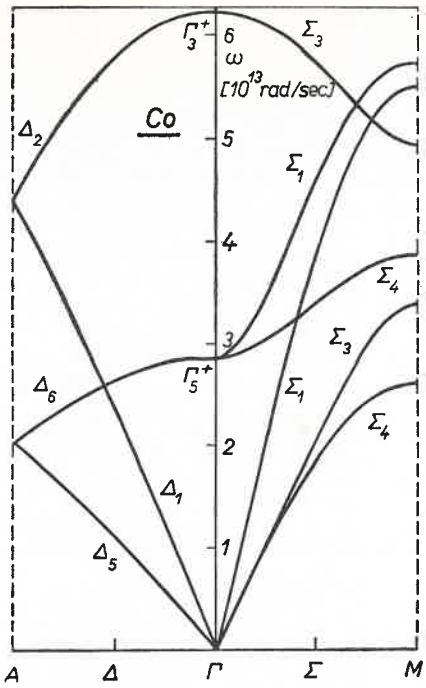

Fig. 4. Model calculated phonon dispersion curves in the directions Δ and Σ for Co

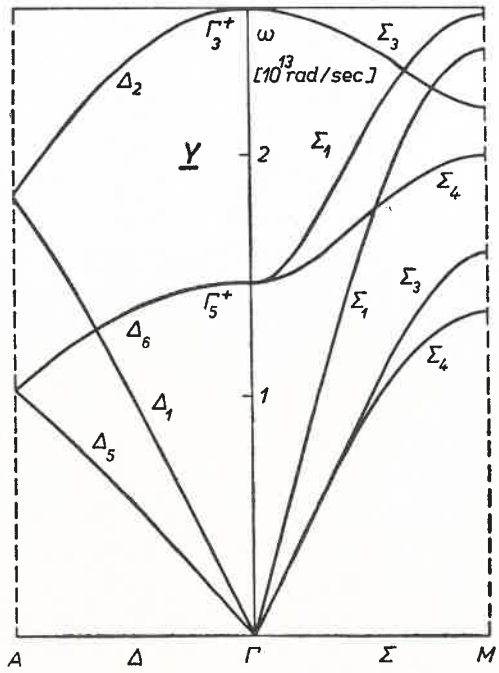

Fig. 5. Model calculated phonon dispersion curves in the directions Δ and Σ for Y

Determination of the phonon frequency spectra

Having developed the model, one is in a position to calculate phonon frequencies and polarization vectors throughout all the Brillouin zone. This information is needed for evaluating many quantities of physical interest. For example, even with a dynamical matrix based on a rather rough model, one obtains polarization vectors and phonon frequencies sufficiently accurately to estimate the dynamical form-factor, necessary for planning the neutron-phonon scattering experiments [2]. Other quantities of this kind are the probability of the Mössbauer effect, particularly in the case of anisotropy [17], or the electron diffuse scattering intensity [16]. The knowledge of the frequency spectrum permits for the calculation of thermodynamic properties of a crystal to be performed [18].

To calculate the frequency spectrum we used the sampling method improved by Gilat and Dolling [19]. In our case the irreducible part of I BZ was divided into a mesh of points, the number of which was about 80. At these points the exact eigenfrequencies and eigenvectors of the dynamical matrix (see Appendix) were computed. Following this, the perturba-

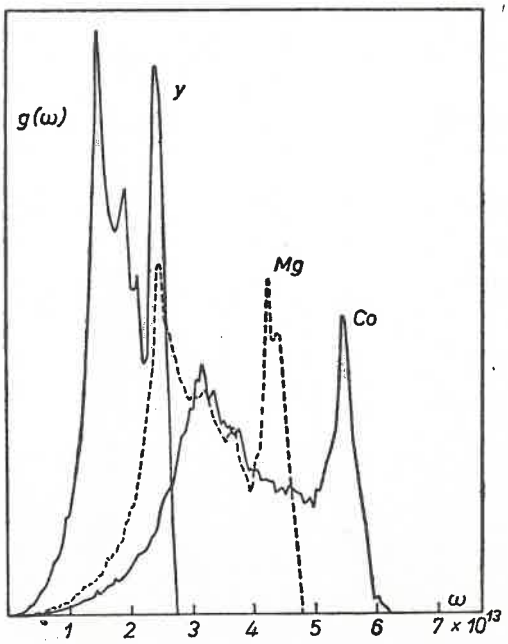

Fig. 6. The averaged phonon frequency distributions for Mg, Co and Y. $\Delta\omega = 5_{10}11$ rad/sec

tion calculations of the frequencies at 125 points, uniformly distributed within a cube about every mesh point, were carried out. Frequencies obtained in this way, usually about 30000 in number were sorted into frequency intervals $\Delta\omega = 5_{10}11$ rad/sec or $\Delta\omega = 1_{10}12$ rad/sec. Every frequency was given a weight (1 or less) following from symmetry considerations. After summing up all the weights in every frequency interval the phonon frequency distribution function (FD) was established.

To avoid, partly at least, the irrelevent peaks in FD due to accidental degeneracies or weight inaccuracies, we repeated all the computations with the mesh of points shifted along the diagonal of a cube by a half of a diagonal, and to add the newly obtained FD-II to the former one, FD-I. The so-obtained "averaged" FD was always smoother than any of the original ones — many small peaks were usually removed. The GIER computer at INR-Świerk was used to perform all the computations.

The averaged frequency distribution for Mg, computed on the assumption $f = 0$ is shown in Fig. 6. The quality of this result is lower than that obtained by Raubenheimer and Gilat [20], as the mesh in their work was much denser than ours, resulting in better accuracy and resolution.

Besides the quality, both slopes differ also in their physical content. In our case the peak at $\omega = 2.5_{10}13$ rad/sec is the highest, whereas they obtained in this region only a maximum, much lower and broader, with some structure. This is, of course, due to the differences

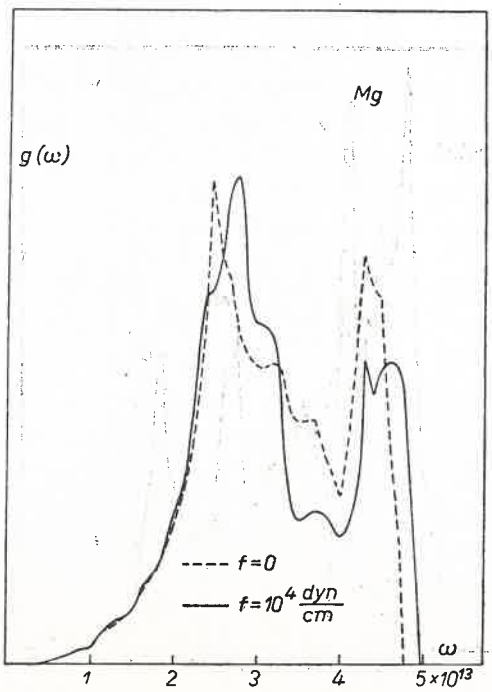

Fig. 7. The phonon frequency distribution FD—I, for Mg, assuming $f = 0$ and $f = 10^4$ dyn/cm; $\Delta\omega = 10^{12}$rad/sec

in the models used. Raubenheimer and Gilat rely on the four neighbours, tensor-force model of Iyengar *et al.* [2], which at first sight seems better in every respect than ours, because it was fitted to a larger number of experimental data. However, it predicts a near degeneracy of two frequencies at point M (see [20]), which disagrees with experimental phonon data. There is no such effect in our model. Also at point K the present model clearly fits the experimental data better. For these reasons we found it interesting to determine

the frequency distribution for Mg also within the present model. However, to obtain a fully reliable FD, one should repeat the computations with still better models, starting perhaps with the one given by Squires [19].

Fig. 6 shows the averaged FD's also for Co and Y. It is interesting to note that the distributions cannot be obtained one from another by any ω-scalling. In the case of Co the total number of frequencies to be sorted was relatively lower, for the $(0, \omega_{max})$ range is in this case the longest. That is why in the case of Co even the "averaging" procedure did not remove many of the obviously accidental peaks.

The tables of polarization vectors and phonon frequencies corresponding to the mesh points are given in [22].

Antisymmetric, many-body force constant cannot be determined from the phonon data for symmetry directions. It seems that this quantity has never been studied systematically. As it does not appear in the expressions for elastic constants, it cannot influence the low-frequency part of FD, and therefore the low-temperature thermodynamic properties of crystals.

The unaveraged, FD-I slopes for Mg are shown in Fig. 7. Frequency distributions for $f = {}_{10}3$ dyn/cm and $f = 0$ are practically indistinguishable. The $f = {}_{10}4$ dyn/cm FD is already modified a much, excepting at the low frequency range. The main peaks became broader and shifted to the right. The ω_{max} increased considerably, as compared with the $f = 0$ case. This means that highest frequencies occur in this case at the points of the I BZ, which do not lie along the main symmetry directions.

Discussion

The relative success of the model presented is obviously due to the domination of the short range ion-ion interactions in the lattice dynamics of Mg. We notice (Table III) that $\sum_{\alpha} \Phi_{\alpha\alpha}(1, 1) \simeq \sum_{\alpha} \Phi_{\alpha\alpha}(1, 2)$, *i.e.* this interaction is highly isotropic.

In terms of isotropic, two-body interaction potential $V(r)$, the smallness of the force constants b and g $\left(\sim \left(\frac{1}{r}\frac{\partial V}{\partial r}\right)_{r=a}\right)$ suggests, that corresponding ions occupy positions very close to the minimum of $V(r)$. This is consistent with the short-range interaction concept. It follows from our estimations, that a simple potential

$$V(r) = \begin{cases} -\delta + \dfrac{\alpha}{2}(r-r_0)^2 & \text{at the two nearest atoms positions,} \\ 0 & \text{besides,} \end{cases}$$

(where δ, α, and r_0 are adjustable parameters), enables one to reproduce the experimental phonon curves for Mg with the accuracy $\sim 8\%$. By allowing a small anisotropy in the potential, one could probably obtain an even better agreement. The parameter δ can be determined from cohesion energy.

It follows from the present work that for Mg, and perhaps for Co and Y, most of the information concerning the form of the microscopic interactions can be deduced from

TABLE IV

Averaged phonon frequency spectrum for Mg

$\Delta\omega = 5_{10}11$ rad/sec, $\Sigma_i g(\omega_i) = 1$

0.000 ,	$1.149_{10}-3$,	$8.748_{10}-3$,	$1.776_{10}-2$,	$1.052_{10}-2$,
0.000 ,	$1.474_{10}-3$,	$8.935_{10}-3$,	$1.801_{10}-2$,	$1.259_{10}-2$,
$5.380_{10}-6$,	$1.774_{10}-3$,	$9.905_{10}-3$,	$1.747_{10}-2$,	$1.355_{10}-2$,
$6.311_{10}-6$,	$1.873_{10}-3$,	$1.137_{10}-2$,	$1.774_{10}-2$,	$1.605_{10}-2$,
$9.560_{10}-6$,	$2.089_{10}-3$,	$1.295_{10}-2$,	$1.823_{10}-2$,	$2.198_{10}-2$,
$5.753_{10}-5$,	$2.519_{10}-3$,	$1.421_{10}-2$,	$1.780_{10}-2$,	$2.724_{10}-2$,
$5.808_{10}-5$,	$2.348_{10}-3$,	$1.706_{10}-2$,	$1.665_{10}-2$,	$2.236_{10}-2$,
$9.467_{10}-5$,	$2.708_{10}-3$,	$1.909_{10}-2$,	$1.590_{10}-2$,	$2.224_{10}-2$,
$1.374_{10}-4$,	$2.736_{10}-3$,	$2.118_{10}-2$,	$1.540_{10}-2$,	$2.290_{10}-2$,
$1.770_{10}-4$,	$3.231_{10}-3$,	$2.807_{10}-2$,	$1.472_{10}-2$,	$2.322_{10}-2$,
$2.576_{10}-4$,	$3.299_{10}-3$,	$2.843_{10}-2$,	$1.453_{10}-2$,	$1.932_{10}-2$,
$2.693_{10}-4$,	$3.693_{10}-3$,	$2.461_{10}-2$,	$1.387_{10}-2$,	$1.426_{10}-2$,
$3.849_{10}-4$,	$4.733_{10}-3$,	$2.303_{10}-2$,	$1.438_{10}-2$,	$1.120_{10}-2$,
$3.875_{10}-4$,	$4.560_{10}-3$,	$2.230_{10}-2$,	$1.428_{10}-2$,	$8.375_{10}-3$,
$7.616_{10}-4$,	$5.099_{10}-3$,	$2.111_{10}-2$,	$1.500_{10}-2$,	$6.382_{10}-3$,
$6.964_{10}-4$,	$5.078_{10}-3$,	$2.056_{10}-2$,	$1.270_{10}-2$,	$2.124_{10}-3$,
$6.867_{10}-4$,	$5.883_{10}-3$,	$1.916_{10}-2$,	$1.204_{10}-2$,	
$9.918_{10}-4$,	$5.912_{10}-3$,	$1.861_{10}-2$,	$1.145_{10}-2$,	
$1.180_{10}-3$,	$7.416_{10}-3$,	$1.825_{10}-2$,	$1.080_{10}-2$,	
$1.080_{10}-3$,	$7.847_{10}-3$,	$1.733_{10}-2$,	$9.856_{10}-3$,	

TABLE V

Averaged phonon frequency spectrum for Co

$\Delta\omega = 5_{10}11$ rad/sec, $\Sigma_i^{\prime} g(\omega_i) = 1$

0.000 ,	$7.429_{10}-4$,	$3.634_{10}-3$,	$1.669_{10}-2$,	$1.174_{10}-2$,	$8.441_{10}-3$,	$1.198_{10}-3$,
0.000 ,	$7.667_{10}-4$,	$4.132_{10}-3$,	$1.641_{10}-2$,	$1.145_{10}-2$,	$1.007_{10}-2$,	$1.460_{10}-3$,
$1.342_{10}-6$,	$9.245_{10}-4$,	$4.678_{10}-3$,	$1.908_{10}-2$,	$1.163_{10}-2$,	$9.866_{10}-3$,	$9.189_{10}-4$,
$1.825_{10}-5$,	$9.109_{10}-4$,	$5.014_{10}-3$,	$1.879_{10}-2$,	$1.071_{10}-2$,	$1.084_{10}-2$,	$6.668_{10}-4$,
$1.552_{10}-5$,	$1.056_{10}-3$,	$4.997_{10}-3$,	$2.045_{10}-2$,	$1.094_{10}-2$,	$1.179_{10}-2$,	$4.195_{10}-4$,
$3.500_{10}-5$,	$1.278_{10}-3$,	$5.058_{10}-3$,	$1.964_{10}-2$,	$1.087_{10}-2$,	$1.256_{10}-2$,	$2.022_{10}-5$,
$4.841_{10}-5$,	$1.296_{10}-3$,	$5.702_{10}-3$,	$1.734_{10}-2$,	$1.059_{10}-2$,	$1.336_{10}-2$,	
$2.286_{10}-5$,	$1.425_{10}-3$,	$6.287_{10}-3$,	$1.761_{10}-2$,	$1.078_{10}-2$,	$1.406_{10}-2$,	
$6.749_{10}-5$,	$1.333_{10}-3$,	$6.531_{10}-3$,	$1.828_{10}-2$,	$9.857_{10}-3$,	$1.568_{10}-2$,	
$3.918_{10}-5$,	$2.046_{10}-3$,	$7.135_{10}-3$,	$1.649_{10}-2$,	$1.008_{10}-2$,	$1.914_{10}-2$,	
$8.341_{10}-5$,	$1.661_{10}-3$,	$8.218_{10}-3$,	$1.532_{10}-2$,	$1.028_{10}-2$,	$2.414_{10}-2$,	
$1.944_{10}-4$,	$1.849_{10}-3$,	$9.305_{10}-3$,	$1.571_{10}-2$,	$9.599_{10}-3$,	$2.359_{10}-2$,	
$2.293_{10}-4$,	$2.222_{10}-3$,	$9.742_{10}-3$,	$1.502_{10}-2$,	$1.046_{10}-2$,	$1.905_{10}-2$,	
$2.078_{10}-4$,	$2.468_{10}-3$,	$1.025_{10}-2$,	$1.531_{10}-2$,	$1.022_{10}-2$,	$1.466_{10}-2$,	
$3.496_{10}-4$,	$2.420_{10}-3$,	$1.038_{10}-2$,	$1.451_{10}-2$,	$9.951_{10}-3$,	$1.254_{10}-2$,	
$3.575_{10}-4$,	$2.939_{10}-3$,	$1.169_{10}-2$,	$1.438_{10}-2$,	$9.745_{10}-3$,	$1.009_{10}-2$,	
$4.599_{10}-4$,	$2.728_{10}-3$,	$1.269_{10}-2$,	$1.505_{10}-2$,	$9.714_{10}-3$,	$8.775_{10}-3$,	
$4.154_{10}-4$,	$2.838_{10}-3$,	$1.427_{10}-2$,	$1.392_{10}-2$,	$8.860_{10}-3$,	$7.465_{10}-3$,	
$5.860_{10}-4$,	$3.133_{10}-3$,	$1.454_{10}-2$,	$1.244_{10}-2$,	$8.971_{10}-3$,	$5.436_{10}-3$,	
$6.336_{10}-4$,	$3.395_{10}-3$,	$1.526_{10}-2$,	$1.145_{10}-2$,	$9.492_{10}-3$,	$2.531_{10}-3$,	

TABLE VI

Averaged phonon frequency spectrum for Y

$\Delta\omega = 5_{10}11$ rad/sec, $\Sigma_i g(\omega_i) = 1$

0.000 ,	$8.080_{10}-3$,	$3.033_{10}-2$,
$1.493_{10}-5$,	$9.249_{10}-3$,	$2.643_{10}-2$,
$4.849_{10}-5$,	$1.098_{10}-2$,	$2.642_{10}-2$,
$7.935_{10}-5$,	$1.304_{10}-2$,	$2.774_{10}-2$,
$1.314_{10}-4$,	$1.431_{10}-2$,	$2.377_{10}-2$,
$3.560_{10}-4$,	$1.757_{10}-2$,	$2.038_{10}-2$,
$4.504_{10}-4$,	$2.109_{10}-2$,	$2.125_{10}-2$,
$7.935_{10}-4$,	$2.551_{10}-2$,	$2.803_{10}-2$,
$8.087_{10}-4$,	$3.118_{10}-2$,	$3.914_{10}-2$,
$1.312_{10}-3$,	$3.863_{10}-2$,	$4.473_{10}-2$,
$1.645_{10}-3$,	$4.765_{10}-2$,	$4.214_{10}-2$,
$2.077_{10}-3$,	$4.364_{10}-2$,	$3.770_{10}-2$,
$2.311_{10}-3$,	$3.869_{10}-2$,	$2.229_{10}-2$,
$2.914_{10}-3$,	$3.503_{10}-2$,	$1.276_{10}-2$,
$3.388_{10}-3$,	$3.299_{10}-2$,	$1.800_{10}-3$,
$4.342_{10}-3$,	$3.155_{10}-2$,	
$4.664_{10}-3$,	$3.112_{10}-2$,	
$5.332_{10}-3$,	$3.240_{10}-2$,	
$6.173_{10}-3$,	$3.240_{10}-2$,	
$7.921_{10}-3$,	$3.487_{10}-2$,	

the elastic constants. It seems possible, that the "first principles" theories of lattice dynamics for the hcp metals [9, 10] could be successfully adapted to the case of Co and Y, by varying their adjustable parameters to fit the theory and experiment at the acoustic limit only.

Note added in proof: The presented phonon dispersion curves for ytrium show a qualitative agreement with the recently published experimental phonon data of S. K. Sinha *et al.* (*Phys. Rev.* **B**1, 2430 (1970)).

APPENDIX

Elements of dynamical matrix

$$md_{11}(\vec{q}) = 3 \cdot B + 3 \cdot (a+b) - 2 \cdot a \cdot \cos(2k_x) - (a+3b) \cdot \cos(k_x) \cdot \cos(k_y)$$

$$md_{22}(\vec{q}) = 3 \cdot B + 3(a+b) - 2b \cdot \cos(2k_x) - (3a+b) \cdot \cos(k_x) \cdot \cos(k_y)$$

$$md_{33}(\vec{q}) = 6 \cdot G - 2 \cdot g \cdot (3 - \cos(2k_x) - 2 \cdot \cos(k_x) \cos(k_y))$$

$$md_{12}(\vec{q}) = \sqrt{3} \cdot (a-b) \cdot \sin(k_x) \cdot \sin(k_y) + i \cdot 2f \cdot (\sin(2k_x) - 2 \cdot \sin(k_x) \cdot \cos(k_y))$$

$$md_{13}(\vec{q}) = md_{23}(\vec{q}) = 0$$

$$mD_{11}(\vec{q}) = -3 \cdot B \cos(k_z) \cdot \cos(k_x) \cdot e^{i(k_z - k_y)}$$

$$mD_{22}(\vec{q}) = -B \cdot \cos(k_z) \cdot (2 \cdot e^{ik_z} + \cos(k_x) \cdot e^{i(k_z - k_y)})$$

$$mD_{33}(\vec{q}) = -2 \cdot G \cdot \cos(k_z) \cdot (e^{ik_z} + 2 \cdot \cos(k_x) \cdot e^{i(k_z - k_y)})$$

$$mD_{12}(\vec{q}) = i \cdot \sqrt{3} \cdot B \cdot \cos(k_z) \cdot \sin(k_x) \cdot e^{i(k_z - k_y)}$$

$$mD_{13}(\vec{q}) = -2 \cdot \sqrt{3} \cdot D \cdot \sin(k_z) \cdot \sin(k_x) \cdot e^{i(k_z - k_y)}$$

$$mD_{23}(\vec{q}) = i \cdot 2 \cdot D \cdot \sin(k_z) \cdot (e^{ik_z} - \cos(k_x) \cdot e^{i(k_z - k_y)})$$

$$k_x = \pi a q_x \qquad k_y = \sqrt{3}\pi a q_y \qquad k_z = \pi c q_z$$

$$D_{\alpha\beta}(\vec{q}|11) = D^*_{\beta\alpha}(\vec{q}|11) = D^*_{\alpha\beta}(\vec{q}|22) = d_{\alpha\beta}(\vec{q})$$

$$D_{\alpha\beta}(\vec{q}|12) = D_{\beta\alpha}(\vec{q}|12) = D^*_{\alpha\beta}(\vec{q}|21) = D_{\alpha\beta}(\vec{q}).$$

REFERENCES

[1] R. E. Schmunk, R. M. Brugger, P. D. Randolph, K. A. Strong, *Phys. Rev.*, **128**, 526 (1962).
[2] P. K. Iyengar, G. Venkateraman, R. P. Vijayaranghavan, A. P. Roy, *Inel. Scatt. Neutr.* (IAEA, Vienna), 1965, I, p. 153.
[3] P. Pynn, G. L. Squires, *Inel. Scatt. Neutr. Sol. Liquids*, (IAEA, Vienna), 1968, I, p. 215.
[4] E. Maliszewski, J. Rosolowski, D. Sledziewska, A. Czachor, *Lattice Dynamics*, Perg. Press 1965, p. 33.
[5] G. Borgonovi, G. Cagliotti, J. J. Antal, *Phys. Rev.*, **132**, 638 (1963).
[6] L. J. Slutsky, C. W. Garland, *J. Chem. Phys.*, **26**, 787 (1957).
[7] R. P. Gupta, B. Dayal, *Phys. Status Solidi*, **7**, 379 (1965).
[8] A. Czachor, *Phys. Status Solidi*, **29**, 423 (1968).
[9] E. G. Brovman, Yu. Kagan, A. Holas, *Inel. Scatt. Neutr. Sol. Liquids* (IAEA, Vienna), 1968, I, p. 153.
[10] G. Giliat, R. Rizzi, G. Cubiotti, *Phys. Rev.*, **185**, 971 (1969).
[11] G. Champier, G. Touissant, *Lattice Dynamics*, Perg. Press 1965.
[12] A. Czachor, *Inel. Scatt. Neutr. Sol. Liquids* (IAEA, Vienna), 1965, p. 181.
[13] G. L. Squires, *Proc. Roy. Soc.*, **88**, 919 (1966).
[14] H. B. Huntington, *Solid State Phys.*, **7**, (1958).
[15] J. F. Smith, J. A. Gjeore, *J. Appl. Phys.*, **31**, 645 (1960).
[16] E. M. Horl, *Optik*, **27**, 99 (1968).
[17] Yu. Kagan, *Dokl. Akad. Nauk SSSR*, **140**, 794 (1961).
[18] A. A. Marachudin, E. W. Montrol, G. H. Weiss, *Solid State Phys.*, Supplement 3, (1963).
[19] G. Gilat, G. Dolling, *Phys. Letters*, **8**, 304 (1964).
[20] L. J. Raubenheimer, G. Gilat, *Phys. Rev.*, **157**, 586 (1967).
[21] A. Czachor, Report INR. nr 1189/II/PS.
[22] A. Czachor, A. Rajca, Report INR nr 1219/II/PS.